Biophysical Journal, Volume 99

Supporting Material

Cholesterol-Dependent Nanomechanical Stability of Phase-Segregated Multicomponent Lipid Bilayers

Ruby May A. Sullan, James K. Li, Changchun Hao, Gilbert C. Walker, and Shan Zou

Supporting Material

Cholesterol-Dependent Nanomechanical Stability of Phase-Segregated Multicomponent Lipid Bilayers

Ruby May A. Sullan,[†‡] James K. Li,[‡] Changchun Hao,[†] Gilbert C. Walker,[‡] and Shan Zou,[†*]

[†]Steacie Institute for Molecular Sciences, National Research Council Canada, Ottawa, Canada;
[‡]Department of Chemistry, University of Toronto, Toronto, Canada

* To whom correspondence should be addressed; email: Shan.Zou@nrc-cnrc.gc.ca

Scheme S1 Typical force curves and schematic illustration of a breakthrough event of a supported lipid bilayer indented by an AFM tip. In the non-contact region *(O-A)*, the tip is far from the surface and the force remains constant. At the contact point *(A)*, the tip starts to contact the lipid surface and continues to indent into it *(A-B),* followed by a sudden breakthrough *(B-C)* of the bilayer with sufficient load. The tip reaches the supporting substrate (*C*) after which the cantilever itself begins to deflect *(C-D)*.

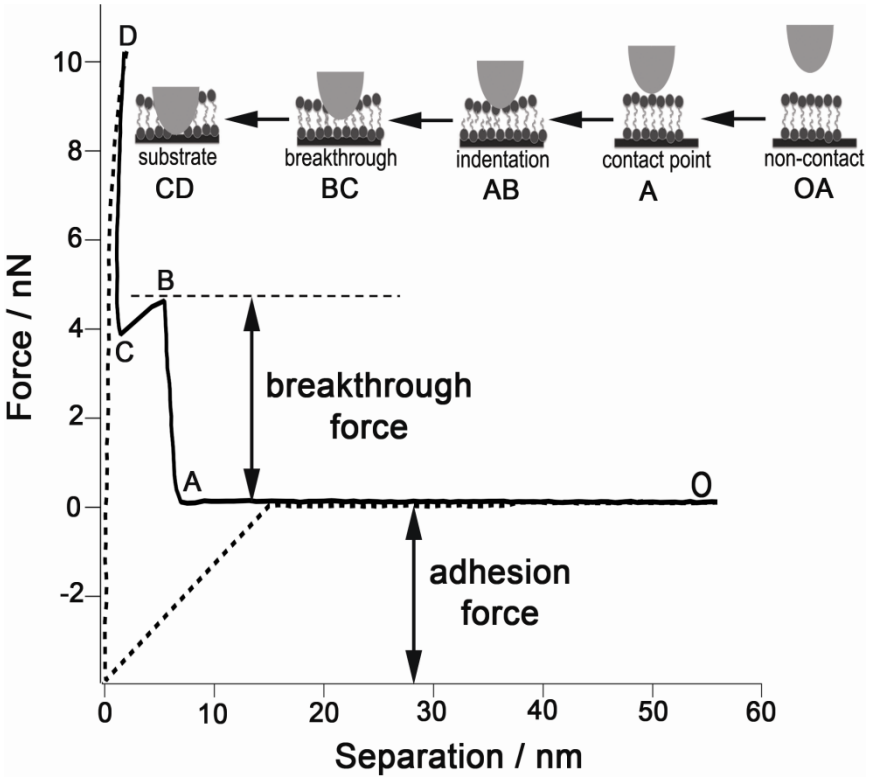

Rupture Activation Energy Calculation

We use the (universal) rupture kinetics model introduced by Butt et al. to calculate the activation energy (ΔE_a) of rupturing lipid membranes (1,2). Below is a brief summary of the calculations.

Consider an ensemble of N_0 simultaneous, identical AFM tip-film indentation experiments occurring at a constant tip loading rate v (loading rate is calculated using the approaching velocity of the base of the cantilever). Let N be the number of films that remain intact after time t has elapsed. Time is referenced to $t=0$, the point at which tip-sample contact begins. The change in number of intact layers dN after time dt can be expressed as:

$$dN = -k_r N dt \qquad (S1)$$

where k_r is a time-dependent constant. Dividing by N_0, Eq. S1 is converted to:

$$dP = -k_r(t) P dt \qquad (S2)$$

where $P=N/N_0$ is the probability of finding a tip on top of the intact film. Integrating Eq. S2,

$$\ln P(t) = -\int_0^t k_r(t')dt' \qquad (S3)$$

Assuming that the rate constant is associated with an activated process following an Arrhenius Law:

$$k_r(t) = Ae^{-\frac{\Delta E_a(F)}{k_B T}} \qquad (S4)$$

where ΔE_a is the activation energy necessary for the formation of a hole or fracture in the film that is large enough to initiate rupture and let the tip break through, F is the yield force, k_B is Boltzmann's constant, T is the Kelvin temperature, and A is the frequency at which the tip attempts to penetrate the film.

Time is transformed to force, using the latter's relation with loading rate

$$F = kvt \qquad (S5)$$

where k is the tip spring constant. Combining Eq. S3-S5

$$\ln P(F) = -\frac{A}{kv}\int_0^F e^{-\frac{\Delta E_a(F')}{k_B T}} dF' \qquad (S6)$$

The probability distribution that this creates represents the distribution of yield forces. If this distribution is narrow, then at the mean yield force F_0, the probability $P(F)$=0.5. With ln(0.5)= -0.693, Eq. S6 can be rewritten:

$$v = \frac{A}{0.693k}\int_0^{F_0} e^{-\frac{\Delta E_a(F')}{k_B T}} dF' \qquad (S7)$$

$$\Delta E_a(F_0) = -k_B T \ln\left(\frac{0.693k}{A}\frac{dv}{dF_0}\right) \qquad (S8)$$

If the $v(F_0)$ relationship is known then its derivative can be calculated to obtain activation energy's dependence on yield force. This is a useful equation, as v and F_0 are experimental observables.

In the case where the distribution of mean breakthrough forces is relatively narrow ($\Delta F/F_0 << 1$, where ΔF is the half width of the yield force distribution), F_0 can be obtained from the histogram of breakthrough forces; the loading rate demonstrates a logarithmic dependence on the breakthrough force, namely,

$$F_0 = a + b\ln v \qquad (S9)$$

where a and b can be derived from geometric parameters and mechanics arguments(3), and more importantly are parameters obtained from fits to experimental data, the dependence of activation energy on loading rate can be explicitly expressed as:

$$\Delta E_a(F_0) = k_B T\left[2.30\frac{a - F_0}{b} - \ln\left(\frac{1.60k}{Ab}\right)\right] \qquad (S10)$$

When this relation is extrapolated to zero mean yield force ($F_0 = 0$), it provides the intrinsic activation energy of the lipid membranes.

In our experiments, the probability distribution of forces is the breakthrough force histogram, which shows bimodality corresponding to the two phases (liquid ordered domains, L_o and fluid disordered phase, L_d), in a series of loading rates. In our calculations, we used a k of ~0.25 N/m, a temperature of 296.2 K, and set A equal to the cantilever's resonant frequency under water (~15×10^3 Hz).

Fluorescence Imaging

Epifluorescence images of DOPC/SM/Chol bilayers with various Chol concentrations were obtained using an Olympus 1X81 inverted confocal microscope equipped with a high-resolution CCD camera (CoolSNAP, Photometrics, US), a 100x/1.40 N.A. oil immersion objective (UPlanSApo, Olympus), and a TRITC-WF filter set (Chroma Technology). All measurements were carried out on mica-on-glass substrates fixed to a liquid cell. The samples were kept hydrated at all times.

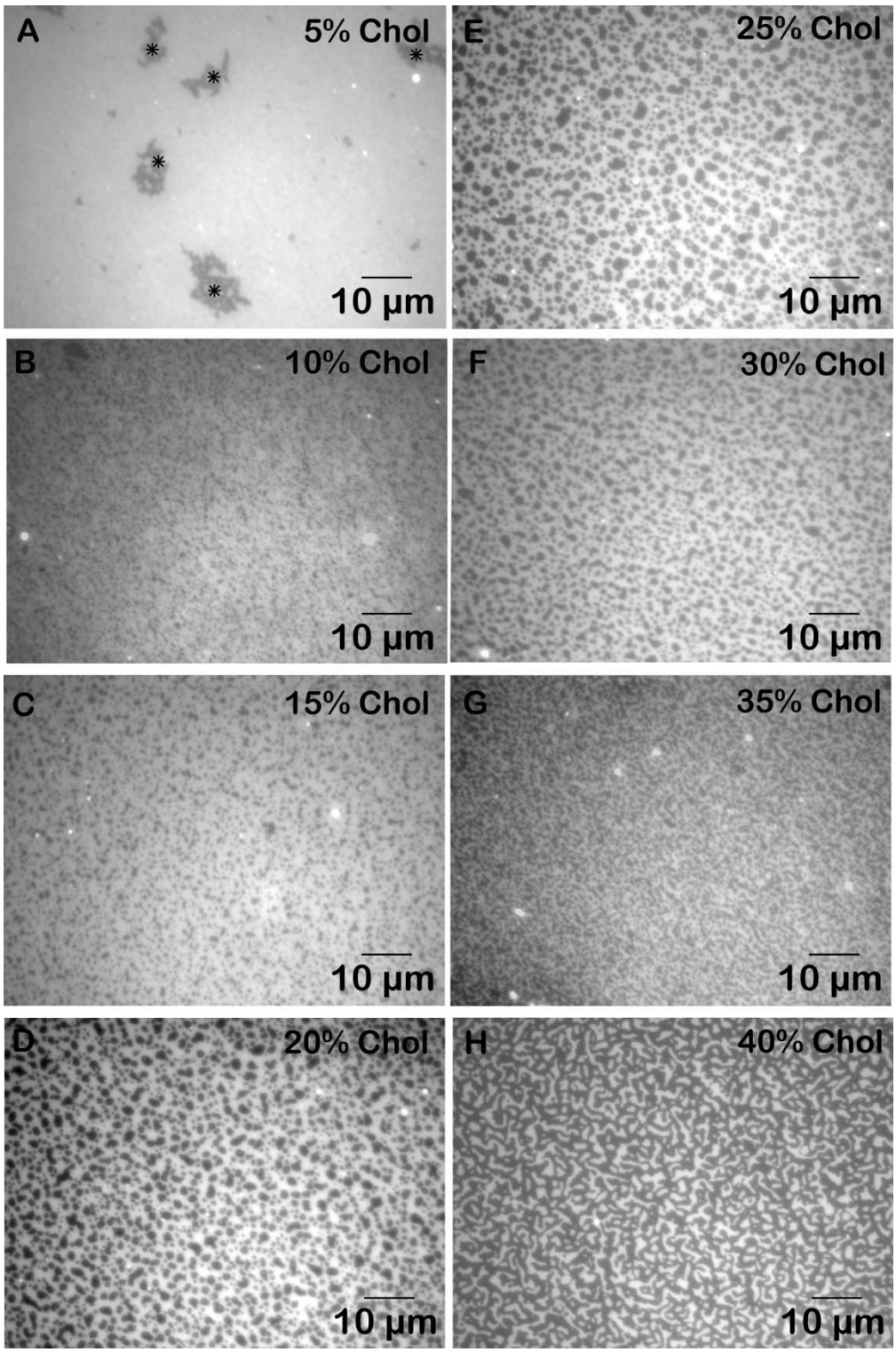

FIGURE S1 Optical images of DOPC/SM/Chol bilayers with 0.3% Texas Red-DHPE at *(A)* 5%, *(B)* 10%, *(C)* 15%, *(D)* 20%, *(E)* 25%, *(F)* 30%, *(G)* 35%, and *(H)* 40% Chol. Images are 88 × 66 μm^2.

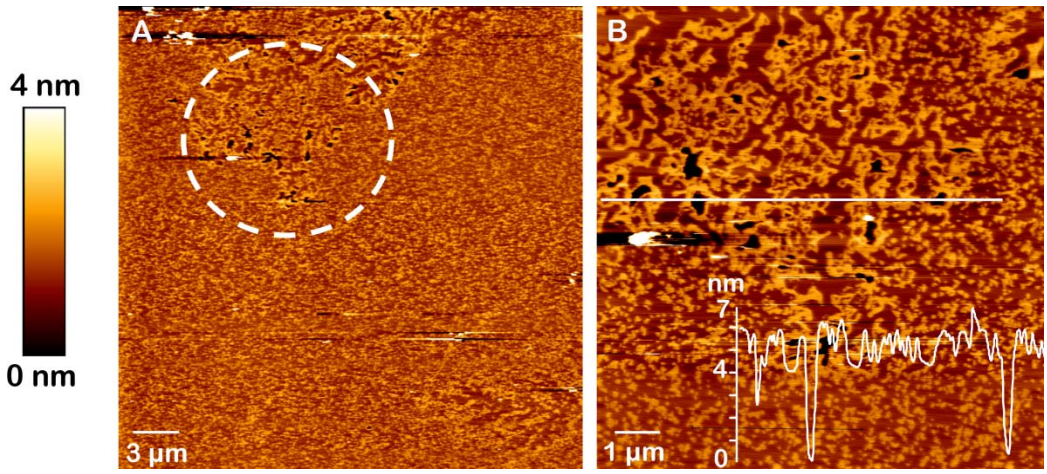

FIGURE S2 AFM height images of DOPC/SM/Chol bilayer with 5% Cholesterol. *(A)* 30 × 30 µm^2 area showing the dark patch also visible in Fig. S1 *A; (B)* 10 × 10 µm^2 of the features within the dashed circle in Fig. S2 *A*. The line profile indicates that the dark patch is a combination of bilayer defects (~ 6 nm) and individual domains that coalesced. Color scale bar at the left side provides z-range.

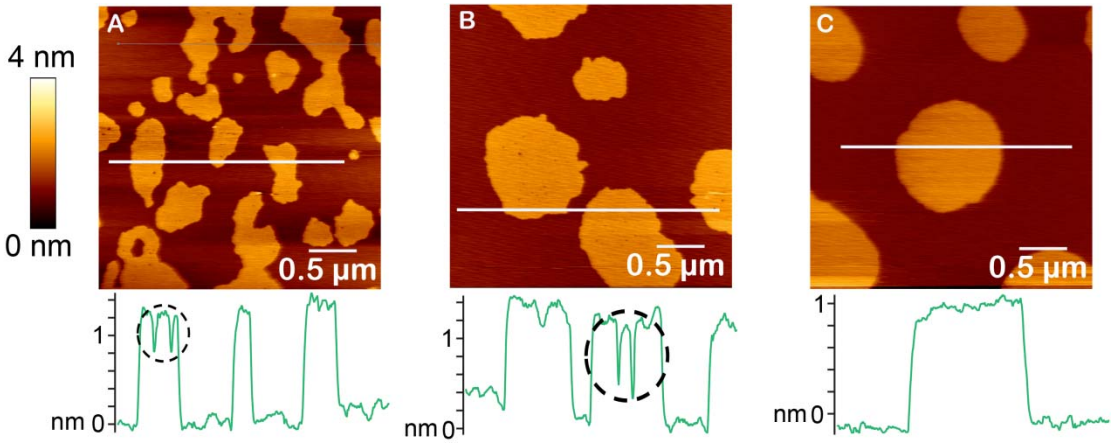

FIGURE S3 AFM height images of of DOPC/SM bilayers with *(A)* 10%, *(B)* 15%, and *(C)* 25% Chol *after* force mapping. The dips/holes (inside the dashed circle) in the line profiles of the bilayers with 10% and 15% Chol indicate the existence of a gel phase. On the contrary, the absence of holes in DOPC/SM with 25% Chol confirms the presence of a liquid ordered state. Color scale bar at the left side provides the z-range.

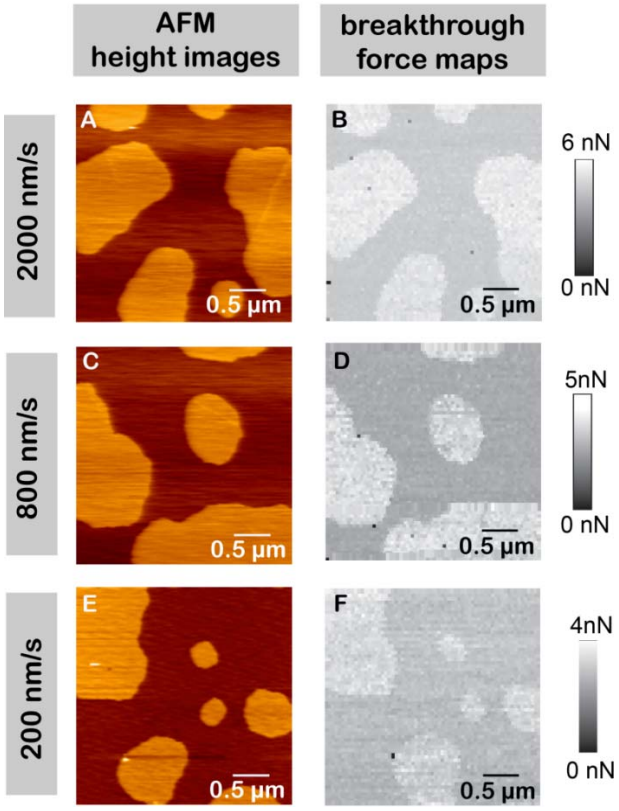

FIGURE S4 Correlated AFM height images and breakthrough force maps of DOPC/SM/Chol bilayers with 20% Chol at (*A, B*) 2000 nm/s, (*C, D*) 800 nm/s, and (*E, F*) 200 nm/s loading rate. It is apparent from these correlated images the lighter regions and the darker matrix in the breakthrough force maps respectively correspond to the L_o and L_d phases.

TABLE S1. Rupture activation energies of the coexisting phases (liquid ordered domains, L_o and fluid disordered phase, L_d in DOPC/SM (1:1) with 10-40% cholesterol bilayers.

Cholesterol Concentration	**Rupture Activation Energy (kJ/mol)**	
	L_d phase	**L_o phase**
10%	73 ± 50	78 ± 123
15%	123 ± 12	93 ± 8
20%	114 ± 23	105 ± 83
25%	73 ± 36	75 ± 28
30%	76 ± 18	85 ± 21
35%	108 ± 15	109 ± 45
40%	85 ± 25	98 ± 74

References:

1. Butt, H. J., and V. Franz. 2002. Rupture of molecular thin films observed in atomic force microscopy. I. Theory. *Phys. Rev. E* 66:031601- 1–9.
2. Loi, S., G. Sun, V. Franz, and H. J. Butt. 2002. Rupture of molecular thin films observed in atomic force microscopy. II. Experiment. *Phys. Rev. E* 66:031602-1–7.
3. Franz, V., S. Loi, H. Muller, E. Bamberg, and H. H. Butt. 2002. Tip penetration through lipid bilayers in atomic force microscopy. *Colloids Surf. B* 23:191-200.